

Performance Prediction of BPN Pyrogen-Type Igniters for Rocket Motors

M. Kuna,* A. Peretz,† and Y. Manheimer-Timnat‡

Department of Aeronautical Engineering, Technion-Israel Institute of Technology, Haifa, Israel

Performance prediction of BPN-charge pyrogen-type igniters by two theoretical methods is presented and compared with experimental results. Using the form function technique, the igniter chamber pressure history is calculated by: 1) an approximate isothermal analytical solution of the theoretical model, and 2) a numerical solution of the more general case. Five different grain configurations and two BPN pyrotechnic compositions have been studied. The grains consist of one, two, or four large pellets bonded in a row. Good agreement between experimental pressure-time records and corresponding solutions of the theoretical model has been obtained. A parametric study, conducted to reveal the effects of some parameters on igniter performance and prediction validity, is presented. The results may be used for design purposes.

Nomenclature

A	= area
a	= coefficient in the burning rate law $r = aP^n$
b	= co-volume
C	= integration constant, see Eq. (5)
c^*	= characteristic velocity
c_d	= nozzle discharge coefficient
D	= diameter
K	= area ratio = A_b/A_i
L	= length of igniter grain
M	= mean molecular weight of igniter combustion products
m	= mass of igniter combustion products
m_0	= initial mass of igniter charge
N	= nondimensional mass, see Eq. (6)
n	= pressure exponent in the burning rate law $r = aP^n$
P	= igniter chamber pressure
R	= specific gas constant of combustion products
r	= burning rate
T	= igniter chamber temperature
T_p	= isobaric flame temperature
T_V	= isochoric flame temperature
t	= time
u	= nondimensional pressure, see Eq. (2)
V	= igniter chamber volume
W	= least burning distance, web
y	= burned distance from propellant surface
Z	= form function – consumed mass fraction, see Eq. (1)
β	= heat loss fraction = $1 - T_{ac}/T_{ad}$
Γ	= a function of $\gamma = \gamma^{0.5} [2/(\gamma + 1)]^{(\gamma + 1)/2(\gamma - 1)}$
γ	= ratio of specific heats
ρ_c	= charge density
σ	= web fraction consumed, see Eq. (1)
ψ	= equivalence ratio

Subscripts

a	= action
ac	= actual
ad	= adiabatic
b	= burning
eff	= effective

i	= igniter chamber; inner (diameter)
m	= maximum
o	= outer
P	= produced
t	= throat
th	= theoretical
0	= values at time $t = 0$

1. Introduction

CONTROL of starting transients of modern solid-propellant rocket motors requires reliable prediction of igniter performance. Pyrogen-type igniters have been preferably used in recent years, because they are more controllable and reproducible than conventional pyrotechnic and hypergolic-type devices, and can improve ignition of rocket motors at extreme environmental conditions.

Pyrotechnic compositions based on boron-potassium nitrate (BPN), unlike conventional solid propellants, have the following advantageous properties: 1) very small dependence of burning rate on pressure; 2) high burning rates at low pressures; 3) good ignitability at subatmospheric pressure; 4) small temperature sensitivity of the burning rate; and 5) radiative and conductive heat transfer modes to the propellant surface to be ignited, due to incandescent particles in the igniter combustion products. The use of BPN pyrotechnic material as a grain in pyrogen-type igniters, thus combining the above-mentioned desirable properties of both groups, has been successfully applied in rocket motor ignition systems. This work describes a performance study of a BPN pyrogen igniter, in which the grain is composed of one or more cylindrical BPN pellets bonded in a row providing a well-defined and predictable development of the burning surface vs burned distance.

Paul and Lovine¹ presented an isothermal analysis of igniter performance and showed that a closed-form analytical solution to the governing ballistic equation exists for certain values of the pressure exponent, n , in the burning rate law. Fair agreement between calculated and measured pressure-time histories was obtained. A similar analysis, conducted by Scheier,² resulted in a more satisfactory fit between calculations and experiments, assuming that the burning rate is independent of pressure. Adams³ calculated iteratively the pressure development in the igniter chamber, without assuming discrete value of n and neglecting mass accumulation in the chamber, heat losses, and discharge coefficient effects.

The theoretical model for igniter internal ballistics, established in this study, relaxes assumptions made by previous investigators. The model was tested by an extensive experimental program, which included determination of the

Presented as Paper 76-670 at the AIAA/SAE 12th Propulsion Conference, Palo Alto, Calif., July 26-29, 1976; submitted Sept. 22, 1976; revision received Dec. 21, 1976.

Index categories: Combustion Stability, Ignition, and Detonation; Fuels and Propellants, Properties of; Solid and Hybrid Rocket Engines.

*Senior Research Engineer. Member AIAA.

†Adjoint Lecturer, Senior Research Engineer. Member AIAA.

‡Professor. Member AIAA.

ballistic and thermodynamic properties of BPN combustion products and firings with different grain configurations and BPN compositions.

II. Theoretical Analysis

The following assumptions for the establishment of the theoretical model are made:

- 1) There are no variations in gas temperature and pressure along the BPN grain.
- 2) The co-volume of the combustion gases is neglected (a good approximation for pressures below 100 atm).
- 3) Igniter nozzles are choked, and deviations from isentropic one-dimensional flow in them are taken into account by a nozzle discharge coefficient.
- 4) There is no erosive burning in the igniter.
- 5) All burning surfaces of the grain ignite uniformly and instantaneously.
- 6) The BPN combustion gases are considered to be ideal.

The geometry of the pyrotechnic charge is described by a form function,^{4,5} which expresses the mass fraction of pyrotechnic material burned, Z , as a cubic function of the web fraction consumed, σ .

$$Z(\sigma) = m_p/m_0 = a_1\sigma + a_2\sigma^2 + a_3\sigma^3 \quad (1)$$

where

$$\sigma = y/W \quad (0 \leq \sigma \leq 1)$$

Using the mass and energy conservation equations for igniter chamber (in accordance with the above-mentioned assumptions), the ideal-gas equation of state, a burning rate law of the form $r = aP^n$, and the form function given by Eq. (1), the following governing equation, relating the dimensionless igniter pressure, u , to σ is obtained:⁶

$$du/d\sigma = f(\sigma) - hu^{1-n} \quad (2)$$

where

$$u = \frac{P}{P_i} \quad f(\sigma) = \frac{dZ}{d\sigma}$$

$$P_i = \frac{(1-\beta)m_0RT_v}{V - m_0/\rho_c}$$

and

$$h = \frac{\gamma\Gamma c_d A_i W P_i^{1-n} T_v^{1/2}}{m_0 a (1-\beta) R^{1/2} T_v}$$

Assuming that the gas temperature in the igniter chamber is constant with respect to time (isothermal analysis), the temperature T in the function h can be replaced by its equilibrium value

$$T_p = T_v(1-\beta)/\gamma \quad (3)$$

For that case, closed analytical solutions to Eq. (2) can be found for three discrete values of the burning rate exponent n : 0, 0.5, and 1. For all other values of n a numerical solution is needed.

In the course of this study it turned out that the closest value of n allowing a closed-form solution for the BPN compositions investigated is $n=0$. In this case Eq. (2) yields a first-order linear differential equation

$$du/d\sigma + hu = f(\sigma) \quad (4)$$

the solution of which is

$$u = C \exp(-h/\sigma) + \frac{1}{h} \left[f(\sigma) - \frac{f'(\sigma)}{h} + \frac{f''(\sigma)}{h^2} \right] \quad (5)$$

Substituting the form function of the specific grain configuration into Eq. (5) and using the initial condition $u(0)=0$, the pressure-time history in the igniter chamber can be obtained. Figure 1 depicts the five grain configurations studied in this work, with their dimensions in millimeters for the four-pellet case. Table 1 lists the respective form functions and analytical solutions.

In order to obtain a numerical nonisothermal solution for any value of n , the basic equations are written in differential form as follows:

mass conservation

$$dN = dZ - \Gamma c_d A_i P dt / m_0 R^{1/2} T^{1/2} \quad (6)$$

where $N = m_i/m_0$

energy conservation

$$T = \frac{T_v(1-\beta)dZ - NdT}{\gamma dZ - (\gamma-1)dN} \quad (7)$$

state

$$P = \frac{Nm_0RT}{V - m_0(1-Z)/\rho_c - bNm_0} \quad (8)$$

burning rate

$$d\sigma = (a/W)P^n dt \quad (9)$$

Using the form function, Eq. (1), this system of equations is solved iteratively by an especially developed Fortran IV computer program. The output of the program contains both the iterative and analytical solutions in tabular, as well as in graphical form.

The BPN data necessary to solve the theoretical model were obtained with the aid of NASA SP-273 computer program⁷ and pertinent experimental data. Two BPN compositions, designated A and B, were studied theoretically and experimentally. The calculated thermodynamic properties of the combustion products at 15 and 30 atm are listed in Table 2.

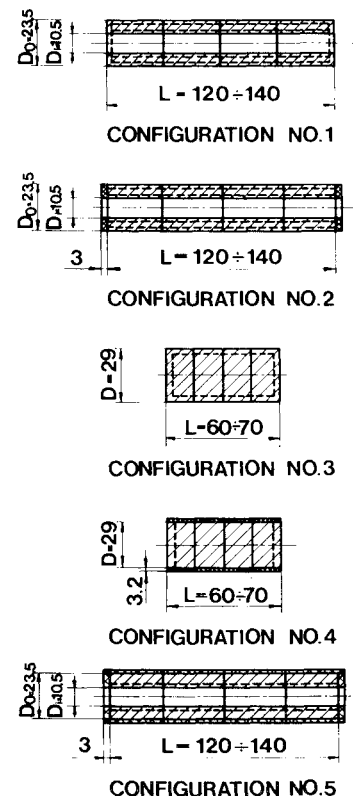


Fig. 1 Grain configurations tested: 1) tubular; 2) tubular with inhibited end surfaces; 3) cylindrical; 4) cylindrical with inhibited side surface; 5) tubular with inhibited end and external side surfaces. Dotted lines show advancing burning surfaces.

Table 1 Form functions and analytical solutions ($n=0$) for the grain configurations studied

Configuration (see Fig. 1)	Form function	Pressure-time relation
1	$Z(\sigma) = -\theta \sigma^2 + (1+\theta)\sigma$ where $\theta = 2W/L$	$P = P_I (\eta/h) [1 - \exp(-hat/W) - 2\theta at/\eta W]$ where $\eta = 2\theta/h + \theta + 1$
2	$Z(\sigma) = \sigma$	$P = (P_I/h) [1 - \exp(-hat/W)]$
3	$Z(\sigma) = \theta \sigma^3 - (1+2\theta)\sigma^2 + (2+\theta)\sigma$	$P = P_I \{ C_I \exp(-hat/W) + (1/h) [3\theta(a/W)^2 t^2 - (1+2\theta+3\theta/h)(2at/W) - C_I h] \}$ where $C_I = -(1/h) [2+\theta+2(1+2\theta)/h+6\theta/h^2]$
4	$Z(\sigma) = \sigma$	$P = (P_I/h) [1 - \exp(-hat/W)]$
5	$Z(\sigma) = \phi \sigma^2 + (1-\phi)\sigma$ where $\phi = (D_0 - D_i)/(D_0 + D_i)$	$P = (P_I/h) [(\Phi - 2)\exp(-hat/W) + 2(\phi at/W + 1) - \Phi]$ where $\Phi = 2\phi/h + \phi + 1$

Table 2 Thermodynamic properties of BPN combustion products

	Composition, %			
	A		B	
Boron	23.6		17.0	
Potassium nitrate	70.9		77.5	
Polyester resin	5.5		5.5	
Eq. ratio, ψ	2.0		1.47	
Property	15 atm	30 atm	15 atm	30 atm
T_p, K	2844	2929	2855	2952
M	59.6	60.8	51.7	52.6
γ	1.112	1.109	1.147	1.145
$c^*_{th}, m/sec$	999	1004	1063	1072

III. Experimental Systems

About 150 igniter tests were conducted in the experimental program. The test set-up comprised the igniter and systems for firing, pressure measurements, and recording. Each igniter consisted of a BPN grain, two initiators, a perforated asbestos-phenolic case, a metallic closure, and an adapter for pressure measurements. An exploded view of a typical igniter is shown in Fig. 2. The pressure in the igniter was measured with a BLH pressure gage and recorded on a Honeywell Visicorder Model 1508A and/or on a Sanborn Model 296 system.

Standard 90-92% purity grade boron with an average particle size of 0.9μ was used in the study. The particle size

spectrum of potassium nitrate was as follows: 27% ranged between 74 and 149μ , 71% between 44 and 74μ , and 2% under 44μ .

The BPN grain is composed of one, two, or four pressed pellets, bonded in a row. The consolidation pressure used was $3,200 \text{ kg/cm}^2$ which resulted in average axial compressive strength of 307 kg/cm^2 for both compositions tested. The weight of each pellet ranged between 19.0 and 20.0 g with an average density of 1.72 g/cm^3 . The parameters changed in each of the five configurations tested were the BPN composition, the ratio K_0 of the initial burning surface to the total nozzle area, and the number of pellets in the grain. The characteristics of the different configurations (see Fig. 1) are:

1) Tubular – provides a slightly regressive development of the burning surface, $A_b(y)$. The values of K_0 used were in the range of 10 to 42.

2) Tubular with inhibited end surfaces – provides a neutral $A_b(y)$. The values of K_0 used ranged as in tests with configuration (1).

3) Cylindrical – provides a regressive $A_b(y)$. Only one value of K_0 , about 30, was used with this configuration.

4) Cylindrical, inhibited on the side surface – provides a neutral $A_b(y)$. The values of K_0 tested were 9.5, 21, and 36.

5) Tubular, inhibited on both end and external side surfaces – provides a progressive $A_b(y)$. The values of K_0 tested ranged from 17 to 25.

IV. Discussion of Results

Typical experimental data from a series of firings carried out with grain configuration No. 1 for the two compositions

Table 3 Typical test data and results for grain configuration No. 1 (four-pellet grain)

Test no.	Grain mass (m_0), g	Grain length (L), mm	Area ratio ($K_0 = A_{b0}/A_I$)	Effective time (t_{eff}), msec	Action time (t_{ac}), msec	Peak pressure ($P_{m_{abs}}$), atm	Effective pressure ($P_{eff_{abs}}$), atm	Effective burning rate (r_{eff}), mm/sec	Effective charac. veloc. (c^*_{eff}), m/sec	Nozzle area (A_I), mm^2
Composition A										
1	78.5	131.5	25.7	85	115	17.0	15.6	38.2	940	554
2	79.6	133.3	26.0	120	140	16.8	13.1	27.1	1090	554
3	76.0	121.6	24.7	110	130	15.7	13.6	29.5	1081	554
4	76.8	123.2	25.0	115	130	13.7	12.1	28.3	995	554
18	78.55	135.8	27.4	105	120	13.7	12.5	31.0	949	554
Composition B										
41	77.7	133.9	20.4	113	123	14.3	11.4	28.8	1195	735
42	79.7	134.0	20.4	123	135	12.8	10.0	26.4	1113	735
43	79.5	134.0	42.5	105	135	30.0	24.9	31.0	1139	353
44	78.3	134.0	42.5	108	135	29.7	22.7	30.1	1084	353
46	80.0	134.2	29.4	118	140	18.2	15.9	27.5	1176	511

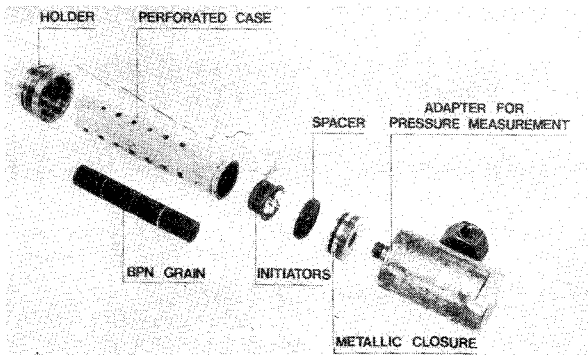
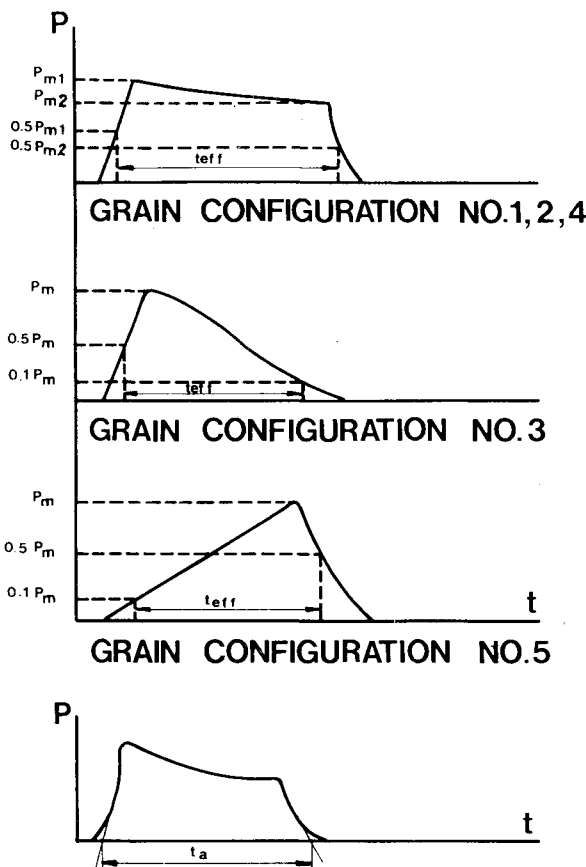


Fig. 2 Exploded view of a typical experimental igniter.

Fig. 3 Definitions of t_{eff} and t_a for the various grain configurations.

tested are given in Table 3. The action and effective times (t_a and t_{eff} , respectively), are defined in Fig. 3. The effective characteristic velocity c_{eff}^* is calculated from the measured igniter pressure integral, namely

$$c_{eff}^* = \frac{A_t}{m_0} \int_0^{t_a} P dt \quad (10)$$

The BPN burning rate law was obtained from data reduction of many pressure-time curves. The results are presented as r_{eff} vs P_{eff} for compositions A and B in Fig. 4. r_{eff} and P_{eff} are defined by dividing the web and the pressure integral, respectively, by t_{eff} . The following burning rate equations, valid at 25°C for the pressure range of 5 to 35 atm, were derived (taking into account all available data by least squares):

composition A

$$r \text{ (cm/sec)} = 2.20P \text{ (atm)}^{0.12}$$

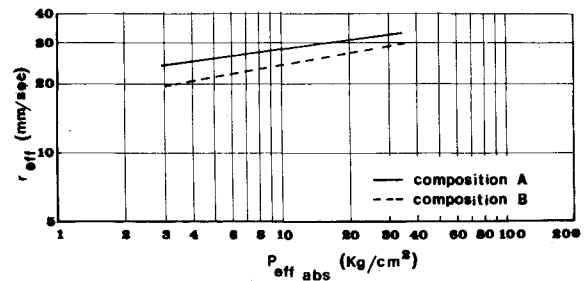


Fig. 4 Experimentally determined effective burning rate vs combustion pressure.

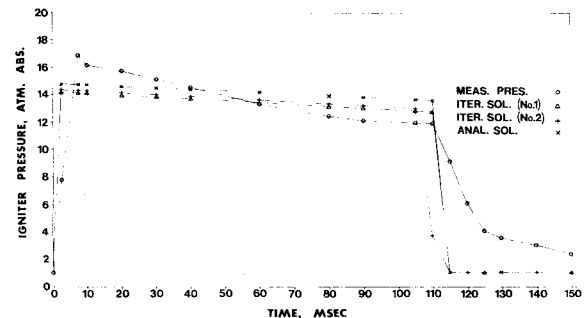


Fig. 5 Comparison of measured and calculated pressure vs time traces obtained with configuration No. 1, four-pellet composition A grain (slightly regressive).

composition B

$$r \text{ (cm/sec)} = 1.63P \text{ (atm)}^{0.20}$$

The calculated adiabatic flame temperature of composition A at 15 atm is 2844 K (see Table 1). An average actual value, T_{ac} , of about 2500 K was measured by Landkopf⁸ in a window igniter motor by optical means. These data yield a value of 0.12 for the heat loss fraction $\beta = 1 - T_{ac}/T_{ad}$, which falls in the range mentioned by Paul and Lovine.¹ The actual characteristic velocity, c_{ac}^* , which is defined as $(RT_{ac})^{1/2}/T$, is accordingly 938 m/sec. An average value of 1020 m/sec was calculated by Eq. (10) for c_{eff}^* from the relevant experimental data; thus, a value of 0.92 is obtained for the discharge coefficient, $c_d = c_{ac}^*/c_{eff}^*$, of the perforated tube nozzles.

Ten to thirty firings at conditioning temperature of $25 \pm 5^\circ\text{C}$ were conducted for each grain configuration and composition. A pressure range of 5 to 35 atm was covered with the above-mentioned changes in K_0 . The burning rate laws used in the analytical solutions ($n=0$) for compositions A and B were $r = 2.86 \text{ cm/sec}$ and $r = 2.73 \text{ cm/sec}$, respectively. These values were determined directly from the experimental results, assuming n to be zero and using again a least-squares fitting.

Two sets of values for the burning rate coefficient and exponent were considered in the numerical solutions, corresponding to tests with composition A: $a_1 = 2.09$ and $n_1 = 0.132$ (iterative solution No. 1, obtained from the experimental r_{eff} vs P_{eff} plot of Fig. 4); $a_2 = 2.24$ and $n_2 = 0.108$ (iterative solution No. 2, obtained from tests with configuration 5, according to the method proposed by Spiegler and Michaeli⁹).

For the numerical solutions comparable to tests with composition B two sets of a and n were again considered as follows: for iterative solution No. 1 - $a_1 = 1.63$ and $n_1 = 0.198$ (obtained from the experimental r_{eff} vs P_{eff} plot of Fig. 4); for iterative solution No. 2 - $a_2 = 1.80$ and $n_2 = 0.180$ (about 10% deviation from solution No. 1). The purpose of using two different sets for a and n was to check the effect of deviations in their values on the pressure-time history prediction.

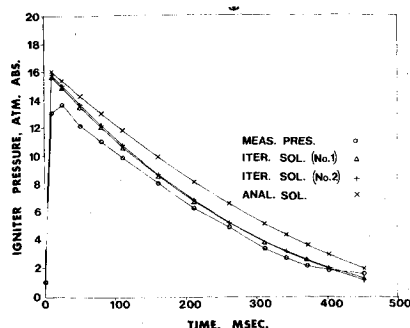


Fig. 6 Comparison of measured and calculated pressure vs time traces obtained with configuration No. 3, four-pellet composition A grain (regressive).

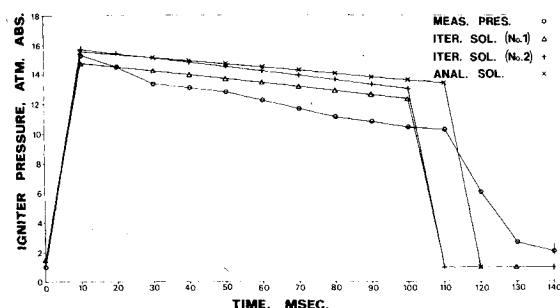


Fig. 7 Comparison of measured and calculated pressure vs time traces obtained with configuration No. 1, two-pellet composition B grain (slightly regressive).

A comparison between typical measured and calculated pressure-time ($P-t$) curves for configuration No. 1 having a four-pellet composition A grain is shown in Fig. 5. Good agreement between the measured and calculated traces is observed. As expected, the numerical solution shows a better fit to the experimental records than the analytical one.

A parametric study has been conducted to reveal effects of various parameters on igniter performance and prediction validity. The effect of boron content on the composition and thermodynamic properties of the combustion gases has been investigated theoretically. For a composition having an equivalence ratio of 0.99 (10% B, 84.5% KNO_3 , and 5.5% polyester) the calculated adiabatic flame temperature and mean molecular weight of the combustion gases at 15 atm are 3053 K and 53.5, respectively. The mole fraction of condensed-phase products for composition A ($\psi=2$) at 15 atm is 0.36 and it decreases to zero as $\psi=1$ is approached, for the same mass fraction of polyester resin. For a stoichiometric B- KNO_3 binary mixture (15.1% B, 84.9% KNO_3) an adiabatic flame temperature and gas mean molecular weight of 3436 K and 61.6, respectively, have been obtained. The effect of pressure on the gas thermodynamic properties is insignificant in the range investigated.

The agreement between calculated and measured $P-t$ traces was almost equally good for all configurations tested. Figure 6 shows a comparison between theory and experiment for configuration No. 3. Again the numerical solution provides a better agreement with experiments.

The number of pellets in the grain affects the igniter performance and prediction usefulness through the effects of grain length-to-diameter ratio. A comparison between calculated and measured $P-t$ curves for configuration No. 1 with a two-pellet composition B grain is shown in Fig. 7. The effect of uninhibited end surfaces on curve regressivity and of

grain length (through A_p/A_t) on erosive burning can be observed, when comparing Fig. 7 with Fig. 5.

The slight deviations of computed $P-t$ curves from the measured ones may be due to one or more of the following factors, which were not accounted for in the theoretical model and input data: erosive burning, noninstantaneous flame spreading over the initial burning surface, eventual break-up of the grain before burnout, two-phase flow effects, impurity of boron, and scatter in BPN properties.

V. Summary and Conclusions

A theoretical model has been established for prediction of BPN igniter performance. About 150 tests with two pyrotechnic compositions, five different grain configurations, and one-, two- and four-pellet grains were carried out to provide experimental verification of pressure vs time theoretical calculations. The solutions of the model presented in this work provide a reliable prediction of the igniter chamber pressure development, irrespective of configuration, composition, number of pellets in the grain, and pressure. Heat losses in the igniter, mass accumulated in the chamber, and an actual discharge coefficient are taken into account. The closed-form analytical solution, which assumes an isothermal process and a zero value for n (close to experimental data), may be used for quick preliminary estimates, whereas the numerical solution provides a more accurate prediction. An important conclusion of this study is that there is no need for very great accuracy in the values of the BPN burning rate coefficient and exponent, in the pressure range tested, in order to obtain satisfactory pressure-time predictions.

It is believed that the results of the study presented contribute to efficient design of pyrogen-type igniters with pyrotechnic grains. The mass flow rate vs time performance of the igniter may be tailored to any ignition energy requirement through the predicted pressure-time dependence.

References

- ¹Paul, B. E. and Lovine, R. L., "Ignition Problems in Solid-Propellant Rockets," *Advances in Tactical Rocket Propulsion*, edited by S. S. Penner, AGARD Conference, Technivision Services, Maidenhead, England, 1968, pp. 195-248.
- ²Scheier, W., "Pressure Transients for Boron Potassium Nitrate Igniters in Inert, Vented Chambers," JPL, Pasadena, Calif., TR No. 32-33, 1960.
- ³Adams, D. M., "Igniter Performance in Solid-Propellant Rocket Motors," *Journal of Spacecraft and Rockets*, Vol. 4, Aug. 1967, pp. 1024-1029.
- ⁴Corner, J., *Theory of the Interior Ballistics of Guns*, Wiley, New York, 1950.
- ⁵Tranter, C. J., "The Form Function," *Internal Ballistics*, edited by R. W. Hunt, G. H. Hinds, C. A. Clemmow, and C. J. Tranter, His Majesty's Stationery Office, London, 1951, pp. 40-52.
- ⁶Kuna, M., Peretz, A., and Manheimer-Timnat, Y., "Parametric Study of a Pyrogen-Type BPN Igniter for Rocket Motors," *Proceedings of the Seventeenth Israel Annual Conference on Aviation and Astronautics*, May 1975, pp. 46-54.
- ⁷Gordon, S. and McBride, B. J., "Computer Program for Calculations of Complex Chemical Equilibrium Compositions, Rocket Performance, Incident and Reflected Shocks, and Chapman-Jouquet Detonations," Lewis Research Center, Cleveland, Ohio, NASA SP-273, 1971.
- ⁸Landkopf, B., "Ballistic Properties of BPN Compositions," Scientific Dept., Ministry of Defense, Israel, TR 135, 1964.
- ⁹Spiegler, E. and Michaeli, E., "Determination of the Interior Ballistic Properties of Solid Propellants from Progressive Burning Grains Data," *Journal of Spacecraft and Rockets*, Vol. 5, May 1968, pp. 623-624.